

## ORIGINAL PAPER

Tomas Radivoyevitch · Rainer K. Sachs  
Yuri E. Nikiforov · Marina N. Nikiforova  
Mark P. Little

## On target cell numbers in radiation-induced *H4-RET* mediated papillary thyroid cancer

Received: 8 February 2001 / Accepted: 11 July 2001

**Abstract** Radiation-induced human papillary thyroid cancer (PTC) is associated with chromosomal inversions that involve the genetic loci *H4* and *RET* on chromosome 10. Recently, experimental data has shown that these loci lie in very close spatial proximity in a high proportion of adult human thyroid cells. Applying the generalized formulation of dual radiation action to this *H4-to-RET* geometric distance data, we predict here the radiation dose-response of *H4-RET* induction. The predicted *H4-RET* dose-response has a linear-to-quadratic transition dose of  $\sim 7$  Gy, suggesting the validity of linear risk extrapolations to very low doses for *H4-RET* mediated radiation-induced PTC. In conjunction with A-bomb survivor data, the predicted *H4-RET* dose-response yields estimates of the number of PTC target cells that are of the order of  $\sim 10^6$  to  $\sim 10^7$  cells, i.e. considerably less than the total number of follicular cells in the thyroid gland.

### Introduction

Recent data [1, 2] suggest that certain gene-pairs, whose juxtaposition in chromosome aberrations may be carcinogenic, sometimes are closer together than would be expected for two typical, uncorrelated locations in the

genome. Previously we modeled the implications of such proximity for a cancer that involves chromosome translocations [3]. Here we model a case that involves chromosome inversions.

Ionizing radiation is associated with thyroid cancer, particularly when exposure occurs at young ages. This claim is supported by a joint analysis of seven externally exposed populations [4] and also by recent studies of internal exposures from the Chernobyl accident [5, 6]. As with spontaneous thyroid cancers [7, 8], most radiation-induced thyroid cancers are of the papillary type [9]. Thus, where thyroid cancer data is not decomposed into its papillary, follicular, anaplastic, and medullary subtypes, it can be assumed that the incidence of papillary thyroid cancer (PTC) approximately equals the incidence of all thyroid cancers combined.

There are associations between PTC and several types of rearrangements of the *RET* proto-oncogene located on chromosome 10q11.2. The two most common types of rearrangement, *RET/PTC1* and *RET/PTC3*, are intrachromosomal inversions. *RET/PTC1* is formed by fusion of *RET* with the *H4* gene [10], and *RET/PTC3* is a product of *RET* fusion with the *ELE1* (*RFG*) gene [11, 12]. The prevalence of *RET* inversions in spontaneous PTCs is less than 10% in Saudi Arabia and Germany [13, 14] and about 30–40% in Japan and parts of the U.S. [15, 16]. In populations exposed to radioactive iodine from the Chernobyl accident the prevalence is as high as 60–80% [17, 18]. *RET* rearrangements have also been detected in 84% of PTCs taken from individuals with a history, in childhood, of external radiation exposures [19, 20]. These numbers suggest that radiation-induced PTC is perhaps due to radiation-induced *RET* rearrangements.

There is strong evidence in mice [21] and in humans [22, 23] that *ELE1-RET* inversions are associated with a solid variant of PTC (follicles filled with cells) that is aggressive and likely to have a short latency time. Consistent with this notion, *RET* rearrangements measured most recently in the Chernobyl region now tend to involve the *H4* locus, rather than *ELE1* [24, 25], suggest-

---

T. Radivoyevitch (✉)  
Department of Epidemiology and Biostatistics,  
Case Western Reserve University Cleveland, OH 44106, USA  
e-mail: radivot@hal.cwru.edu  
Tel.: +1-216-368-1965, Fax: +1-216-368-1969

R.K. Sachs  
Department of Mathematics, University of California, Berkeley,  
CA 94720, USA

Y.E. Nikiforov · M.N. Nikiforova  
Department of Pathology, University of Cincinnati, Cincinnati,  
OH 45267, USA

M.P. Little  
Department of Epidemiology and Public Health,  
Imperial College School of Science, Technology and Medicine,  
London W2 1PG, UK

ing that perhaps the early induced *ELE1-RET* cases are “washing-out” as late arriving *H4-RET* cases begin to take over.

Transgenic mice studies support the notion that *H4-RET* (*RET/PTC1*) is sufficient to initiate PTC [26, 27]. Expressing the *H4-RET* chimeric gene under the control of a thyroid-specific promoter, these mice develop bilateral PTCs that are similar to human PTCs in that they are indolent, only locally invasive, and characterized by diagnostic cytological features that include nuclear grooves, pseudo-inclusions, and ground glass nuclei. In addition, *H4-RET* has been found in many occult (<1 cm in size) PTCs [28]. These results suggest that *H4-RET* may be an early event in thyroid carcinogenesis.

Based on the recent change in relative prevalence of *ELE1-RET* (*RET/PTC3*) and *H4-RET* (*RET/PTC1*) in PTCs associated with of Chernobyl accident [24, 25], we assume that most radiation-induced PTCs arriving 12–35 years after an exposure are mediated by *H4-RET*. Granting this assumption, and assuming further that the PTC incidence is well approximated by the incidence of all thyroid cancers combined, the *H4-RET* dose-response predicted by applying the theory of dual radiation action (TDRA) to recent *H4-to-RET* distance data is related here to the dose-response of thyroid cancer incidence in the Japanese atomic-bomb survivor life span study (LSS) [29]. This relationship leads to estimates of the number of target cells in *H4-RET*-mediated PTC. The estimates suggest that the number of PTC target cells is less than the total number of follicular cells in the thyroid gland.

## Methods

The theory of dual radiation action

To quantify  $E(hr|D)$ , the dose-response of the expected yield of *H4-RET* inversions per cell exposed to dose  $D$ , we will use a loci-specific adaptation [3] of the distance formulation of the theory of dual radiation action (TDRA) [30]. This adaptation of TDRA (see [3] for details) yields:

$$E(hr|D) = \frac{T_{H4}T_{RET}G^2D}{2\Gamma^2} \int_0^\infty \frac{t_D(r)}{\rho 4\pi r^2} S_{hr}(r) g(r) dr \quad (1)$$

$$= \alpha_{hr}D + \beta_{hr}D^2 = \frac{2T_{H4}T_{RET}}{\Gamma^2} (\alpha_{HR}D + \beta_{HR}D^2)$$

where  $\rho=1$  gm/cm<sup>3</sup> is the mass density,  $r$  is the initial distance between two DSBs,  $t_D(r)dr$  is the expected amount of energy deposited in a spherical shell (volume  $4\pi r^2 dr$ ) centered at an arbitrary energy-weighted ionization point,  $S_{hr}(r)$  is the probability density that *H4* and *RET* are a distance  $r$  apart,  $g(r)$  is the conditional probability that two DSBs misrejoin given that they are created  $r$  units apart, the *H4* target size  $T_{H4}$  is 70 kbp [31], the *RET* target size  $T_{RET}$  is 2 kbp [10], the human genome size  $\Gamma$  is 3200 Mb [32] and  $G=35$  DSBs per Gy per cell during  $G_0/G_1$  [33, 34]. Here  $\alpha_{HR}$  and  $\beta_{HR}$  are a rescaling of  $\alpha_{hr}$  and  $\beta_{hr}$  that allows direct comparisons with literature values of  $\alpha_d$  and  $\beta_d$  for total dicentrics. We will estimate  $S_{hr}(r)$  from recent *H4-to-RET* distances measured in adult human thyroid cells [1] and we will assume  $g(r)$  and  $t_D(r)$  as in previous work [3].

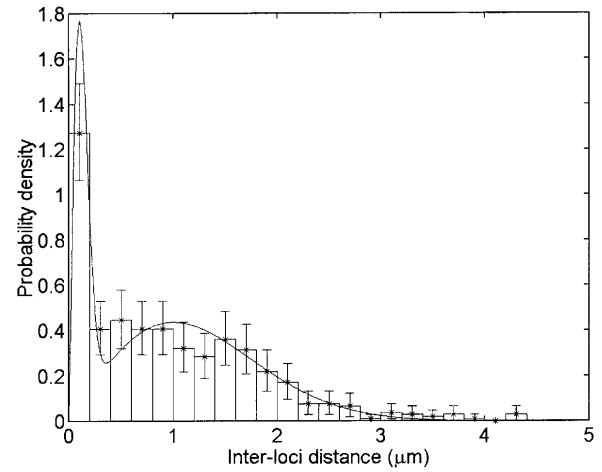


**Fig. 1** The *H4-to-RET* 2D distance distribution in adult human thyroid cells [1]. Distance measurements were grouped into 0.2  $\mu\text{m}$  intervals and the number of distances in each interval divided by the total, 526. Error bars on the data points are 95% CI obtained assuming a Poisson distribution for the counts in each interval. The curve shown (solid line; Eq. 5) was obtained by trial-and-error; the parameter values  $\sigma_s=0.1$   $\mu\text{m}$  and  $p=0.28$  were chosen such that the probability mass between 0 and 0.2  $\mu\text{m}$ , and 0.2 and 0.4  $\mu\text{m}$ , matches the respective two data points, the parameter  $\sigma_f=1$   $\mu\text{m}$  was chosen so that it roughly fits the remaining data points.

Estimation of  $S_{hr}(r)$

The loci *H4* and *RET* lie approximately 30 Mb apart on chromosome 10. Assuming a Gaussian polymer model of chromatin [35], the 3D probability density  $S_{hr}(r)$  becomes:

$$S_{hr}(r) = \frac{\sqrt{2}}{\sqrt{\pi} \sigma^3} r^2 e^{-\frac{r^2}{2\sigma^2}} \quad (2)$$

and the corresponding 2D projections have a Rayleigh distribution:

$$f(r) = \frac{1}{\sigma^2} r e^{-\frac{r^2}{2\sigma^2}} \quad (3)$$

where the scale parameter  $\sigma$  is common to both Eqs. (2) and (3), i.e. fitting 2D data to Eq. (3) is equivalent to fitting the underlying 3D distances to Eq. (2). The observed 2D *H4-to-RET* distance distribution (Fig. 1) does not conform to a Rayleigh distribution – there are too many distances less than 0.4  $\mu\text{m}$  [1]. To model this data, we will assume, much as in [3], that for some percentage of time, or equivalently for our purposes, for some percentage of loci pairs, a “bond” exists such that *H4* and *RET* are tethered to lie within very small distances. This leads to the distance distribution model:

$$S_{hr}(r) = p \frac{\sqrt{2}}{\sqrt{\pi} \sigma_s^3} r^2 e^{-\frac{r^2}{2\sigma_s^2}} + (1-p) \frac{\sqrt{2}}{\sqrt{\pi} \sigma_f^3} r^2 e^{-\frac{r^2}{2\sigma_f^2}} \quad (4)$$

$$f(r) = p \frac{1}{\sigma_s^2} r e^{-\frac{r^2}{2\sigma_s^2}} + (1-p) \frac{1}{\sigma_f^2} r e^{-\frac{r^2}{2\sigma_f^2}} \quad (5)$$

A trial-and-error fit of this model to the 2D data in Fig. 1 (described in more detail in the figure legend) yields  $\sigma_s=0.1$   $\mu\text{m}$ ,  $\sigma_f=1$   $\mu\text{m}$  and  $p=0.28$ . These parameters applied to Eq. (4) give  $S_{hr}(r)$  which, when applied to Eq. (1), provides a TDRA prediction (below) of the *H4-RET* dose-response.

Fits to Japanese atomic bomb survivor data

In the following section we describe a simple empirical model, given by Eq. (6) below, that is fitted to the Japanese atomic bomb

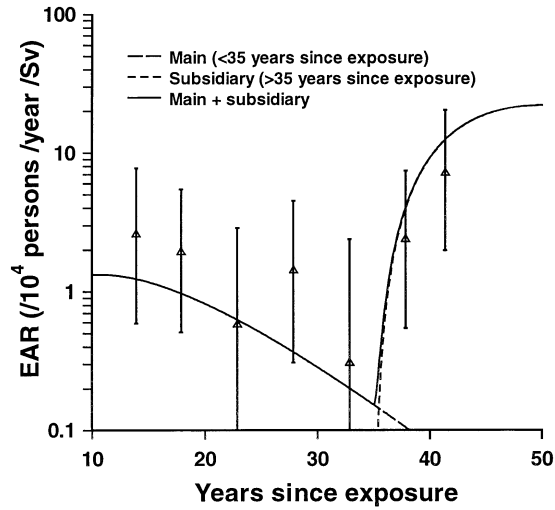


**Fig. 2** The excess absolute risk (EAR) of thyroid cancer among A-bomb survivors, obtained by fitting Eq. (7). The error bars are 95% CI based on the likelihood profiles of  $\exp(L(t))$ . The curves shown correspond to Eq. (8) (the only contribution to EAR up to 35 years after exposure), to Eq. (9) (the subsidiary contribution to EAR, but dominant beyond 35 years after exposure), and to their sum, and are obtained by fitting Eq. (6) by maximum likelihood to the LSS data.

survivor thyroid cancer incidence data. We assume that PTC incidence ( $\approx$ thyroid cancer incidence) consists of a background component (linear in age) and three independent radiation-induced components: an immediately rising, and shortly thereafter falling *ELE1-RET* component, which we do not model in Eq. (6) because its relative contribution to LSS data is expected to be minor (see [24, 25] and note that follow-up in the LSS study began 12.4 years after the exposure); an *H4-RET* component (the focus of this paper) that begins just after the exposure but is negligible after 35 years (i.e. the more solid dashed curve in Fig. 2); and a third component that begins only after 35 years (the more weakly dashed curve in Fig. 2). The model with only the second (*H4-RET*) component fits statistically significantly worse ( $P < 0.001$ ) than the model with both second and third components included, as one would expect from examination of Fig. 2. The second and third components are modeled as a product of an initiation term and a  $\Gamma(3, k)$  waiting-time distribution, which for the third component was translated by 35 years. (We assume *a priori* that this distribution function should begin with zero slope, rise, and then fall back to zero. Our specific choice used here is no more than a simple representative of such functions.) This  $\Gamma(3, k)$  waiting-time distribution provided a good fit to both parts (12.4–35 years after exposure, 35+ years after exposure) of the Japanese data, as can be seen from Fig. 2. The resulting model is:

$$m_i = \left[ e^{c_1 + c_2 \cdot 1_{sex=f}} a_i + (D_{\gamma_i} + RBE \cdot D_{ni}) t_i^2 e^{c_3 + c_4 \cdot 1_{sex=f} - k_{i1} t_i + \lambda_1 x_i} + 1_{t_i > 35} (D_{\gamma_i} + RBE \cdot D_{ni}) (t_i - 35)^2 e^{c_5 + c_6 \cdot 1_{sex=f} - k_{i2} (t_i - 35) + \lambda_2 x_i} \right] P_i \quad (6)$$

where  $m_i$ ,  $a_i$ ,  $x_i$ ,  $P_i$ ,  $t_i$ ,  $D_{\gamma_i}$  and  $D_{ni}$  denote the expected number of PTC cases, the average age at diagnosis, the average age at exposure, the (migration-adjusted) person-years, the average number of years since exposure, and the average gamma and neutron adjusted thyroid doses, respectively, for the  $i$ th grouped epidemiological data cell. Here  $c_1, \dots, c_6$ ,  $\lambda_1$ ,  $\lambda_2$ ,  $k_{i1}$  and  $k_{i2}$  are model parameters to be estimated from the LSS data and  $1_s$  equals one if statement  $s$  is true, zero otherwise. All atomic bomb survivors with shielded kerma dose  $> 4$  Gy were excluded from our analysis because of possible errors in dose estimates at high doses, and because of possible cell-sterilization effects. Consistent with previous analyses [29] and a predicted *H4-RET* linear-to-quadratic transition dose of  $\sim 7$  Gy for  $\gamma$ -rays (see results below), our model assumes linearity in

**Table 1** PTC target cell number estimates for males ( $N_m$ ) and females ( $N_f$ )

$\alpha_{HR\gamma}$ ( $\text{Gy}^{-1}$ )	Neutron RBE	$N_m$ ( $10^7$ cells)	$N_f$ ( $10^7$ cells)
45	20	0.24 [0.048, 1.04] <sup>a</sup>	0.89 [0.33, 2.43]
21	20	0.50 [0.101, 2.21]	1.89 [0.71, 5.17]
45	5	0.27 [0.064, 1.09]	1.00 [0.39, 2.67]
45	80	0.16 [0.024, 0.78]	0.62 [0.22, 1.79]

<sup>a</sup> 95% CI are shown in square brackets.

dose. The data set was stratified by city, sex, time since exposure and age at exposure; this stratification is identical to that employed in the original analyses of this data [29]. As a baseline for our calculations, a neutron relative biological effectiveness (RBE) of 20 was assumed, in accordance with the recommendations of the International Commission on Radiological Protection [36]. The model was fitted by maximum likelihood [37] using MATLAB [38].

#### Time trends in excess absolute risk

In order to estimate excess absolute risk (EAR, Fig. 2) by intervals of time since exposure we fitted the following model

$$m_i = \left[ e^{c_1 + c_2 \cdot 1_{sex=f}} a_i + (D_{\gamma_i} + RBE \cdot D_{ni}) e^{c_4 \cdot 1_{sex=f} + L(t_i) + \lambda x_i} \right] P_i \quad (7)$$

to the LSS data. Here  $L(t)$  is a piecewise constant function of time since exposure  $t$ . The resulting estimates of EAR, given by  $\exp(L(t_i))$ , were obtained using AMFIT [39] and plotted in Fig. 2; 95% confidence intervals (error bars) in this plot were calculated from the profile likelihood [37]. The first of the three curves shown in Fig. 2 is the main component of EAR (per unit dose), and the only component of the excess risk up to 35 years after exposure:

$$EAR_{<35}(t) = t^2 e^{c_3 - k_{i1} t}. \quad (8)$$

This corresponds to the *H4-RET* component of PTC risk (we omit terms adjusting for age at exposure and sex). Also shown in Fig. 2 is the subsidiary component of EAR, which largely dominates the risk 35 or more years after exposure:

$$EAR_{>35}(t) = 1_{t > 35} (t - 35)^2 e^{c_5 - k_{i2} (t - 35)} \quad (9)$$

and the sum of these two components. Implicit in the component of EAR given by Eq. (8) is the *H4-RET*-to-PTC waiting time probability density:

$$w(t) = \frac{k_{i1}^3 t^2}{2} e^{-k_{i1} t} \quad (10)$$

which is a  $\Gamma(3, k_{i1})$  distribution;  $w(t)$  is simply a one parameter summary of all events that occur subsequent to *H4-RET* induction in a target cell.

#### Target cell estimates

In our model  $\alpha_{hr\gamma} [D_{\gamma_i} + RBE \cdot D_{ni}]$  is the probability of forming *H4-RET* in a PTC target cell. Given an estimate of  $\alpha_{hr\gamma}$  based on TDRA, and given estimates of  $c_3$ ,  $c_4$  and  $k_{i1}$  obtained by fitting the LSS data to Eq. (6) [note that these estimates depend on the neutron RBE], we estimate the number of PTC target cells  $N$  (Table 1) as:

$$e^{c_3} = N \alpha_{hr\gamma} \frac{k_{i1}^3}{2} = N \frac{2T_{H4} T_{RET}}{\Gamma^2} \alpha_{HR\gamma} \frac{k_{i1}^3}{2} \Rightarrow N = \frac{\Gamma^2 e^{c_3}}{T_{H4} T_{RET} \alpha_{HR\gamma} k_{i1}^3} \quad (11)$$

for males, and by similar calculations:

$$N = \frac{\Gamma^2 e^{c_3 + c_4}}{T_{H4} T_{RET} \alpha_{HR\gamma} k_{i1}^3} \quad (12)$$

for females. It is assumed here that *H4-RET* formation rate-limits the *H4-RET* component of radiation-induced PTC risk, i.e. that once *H4-RET* is induced in a target cell, *H4-RET*-mediated PTC is destined to follow within about 35 years (in the absence of competing risks). This assumption is implicit in the use of a normalized probability density for  $w(t)$  in Eq. (10).

## Results

The *H4-RET*  $\gamma$ -ray dose-response parameters  $\alpha_{HR\gamma}$  and  $\beta_{HR}$  were predicted by Eq. (1) using  $t_D(r)$  for  $^{60}\text{Co}$   $\gamma$ -rays [40],  $S_{hr}(r)$  defined by Eq. (4) with  $\sigma_s=0.1\ \mu\text{m}$ ,  $\sigma_f=1\ \mu\text{m}$  and  $p=0.28$  and, based on dicentric yields in lymphocytes,  $g(r)=p_0e^{-(r/r_0)}$  with  $r_0=0.24\ \mu\text{m}$  and  $p_0=0.13$  (these assume  $R=3.7\ \mu\text{m}$  [2] for the radius of lymphocyte nuclei, see [3]), or  $r_0=0.26\ \mu\text{m}$  and  $p_0=0.06$  (these assume  $R=3\ \mu\text{m}$  [41]). This gave  $\alpha_{HR\gamma}=44.7\ \text{Gy}^{-1}$  and  $\beta_{HR}=6.5\ \text{Gy}^{-2}$  ( $\alpha_{HR\gamma}/\beta_{HR}\approx 7\ \text{Gy}$ ) for  $R=3.7\ \mu\text{m}$ , which we take as our baseline, and  $\alpha_{HR\gamma}=21.0\ \text{Gy}^{-1}$  and  $\beta_{HR}=3.1\ \text{Gy}^{-2}$  ( $\alpha_{HR\gamma}/\beta_{HR}\approx 7\ \text{Gy}$ ) for  $R=3.0\ \mu\text{m}$ . These  $\alpha_{HR\gamma}$  and  $\beta_{HR}$  values are much higher than  $\alpha_{HR\gamma}=0.26\ \text{Gy}^{-1}$  and  $\beta_{HR}=0.66\ \text{Gy}^{-2}$  ( $\alpha_{HR\gamma}/\beta_{HR}\approx 0.4\ \text{Gy}$ ) obtained assuming no tethering, i.e. assuming  $S_{hr}(r)$  based on Eq. (2) with  $\sigma=1\ \mu\text{m}$ . The intuitive reason  $\alpha$  and  $\beta$  both increase with tethering is that two nearby loci are more likely to interact than are two distant loci; the intuitive reason  $\alpha$  increases even more than  $\beta$  is that two nearby loci are more likely to get DSBs from the same photon than are two distant loci.

Estimates of the number of PTC target cells were formed by applying multivariate normal random samples of  $c_3$ ,  $c_4$  and  $k_{11}$  to Eqs. (11) and (12). The sampling distributions were obtained by fitting Eq. (6) to the LSS data using likelihood-based methods. An overall total of 227 thyroid cancer cases contributed to this estimate. Likelihood optimizations and subsequent simulations were all done in MATLAB [38]. The net results are shown in Table 1 and show that halving  $\alpha_{HR\gamma}$  results in a doubling in  $N$ , see Eqs. (11) and (12), and that decreases in the neutron RBE cause less relative change in  $N$  than increases in the neutron RBE – this happens because, at a neutron RBE of 20, the Sv dose received by the A-bomb survivors is mostly due to  $\gamma$ -rays.

## Discussion

In thyroid cells and lymphocytes, *H4-to-RET* [1] and *BCR-to-ABL* [2] distances, respectively, lie in the range of 0 to  $0.4\ \mu\text{m}$  too frequently to be attributable to chance alone. This suggests the existence of chromosome “bonds” that can tether breakpoint regions into close proximity. The nature of these chromosome bonds, and their significance in radiation-induced carcinogenesis in general, is yet to be determined. If such bonds exist, they would promote putatively carcinogenic misjoining events through two mechanisms: (1) they would increase the probability that one photon creates double strand breaks (DSBs) in both breakpoint regions, and (2), given that the breakpoint regions each have DSBs, they would

increase the probability that such DSBs misrejoin. The theory of dual radiation action (TDRA) represents both of these mechanisms mathematically. It provides loci-specific dose-response predictions (Eq. 1) from a combination of inter-loci distance data (Fig. 1) and microdosimetric exposure descriptions. Importantly, TDRA predicts (here and in [3]) that tethered states cause (and thus explain) linear  $\gamma$ -ray dose-response behavior (for doses  $<4\ \text{Gy}$ ) such as that observed for thyroid cancer [29] and chronic myeloid leukemia (CML) [42].

Suppose *H4* and *RET* were on separate chromosomes and that *H4-to-RET* distance data were not available. Default assumptions for  $\alpha_{HR\gamma}$  and  $\beta_{HR}$  might then have been the literature values for dicentrics,  $\alpha_{d\gamma}=0.01\text{--}0.025\ \text{Gy}^{-1}$  and  $\beta_{d\gamma}=0.05\text{--}0.06\ \text{Gy}^{-2}$  [41, 43]. Knowing, however, that *H4* and *RET* are 30 Mb apart on chromosome 10, a relationship between inter-loci geometric distances and inter-loci genomic distances [35] suggests that  $S_{hr}(r)$  be given by Eq. (2) with  $\sigma$  between  $1.6\ \mu\text{m}$  and  $2.5\ \mu\text{m}$ . Using  $\sigma=1.6\ \mu\text{m}$ , TDRA yields  $\alpha_{HR\gamma}$  and  $\beta_{HR}$  each about threefold higher than for dicentrics. Using  $\sigma=2.5\ \mu\text{m}$ , it yields values about equal to those of dicentrics. Given *H4-to-RET* distance data without tethered states [i.e. Eq. (2) with  $\sigma=1\ \mu\text{m}$ ], TDRA yields  $\alpha_{HR\gamma}$  and  $\beta_{HR}$   $\sim 10$ -fold higher than for dicentrics ( $\sigma < 1.6\ \mu\text{m}$  here is perhaps due to different cell shapes, i.e. round thyroid cells versus flat fibroblasts). Given *H4-to-RET* data with tethered states [i.e. Eq. (4) with  $\sigma_s=0.1\ \mu\text{m}$ ,  $\sigma_f=1\ \mu\text{m}$  and  $p=0.28$ ], TDRA yields  $\alpha_{HR\gamma}$  and  $\beta_{HR}$  about 1000-fold and 100-fold higher, respectively, than  $\alpha_{d\gamma}$  and  $\beta_{d\gamma}$  for dicentrics. In this case,  $\alpha_{HR\gamma}/\beta_{HR}\approx 7\ \text{Gy}$  is substantially higher than the literature range for dicentrics,  $\alpha_d/\beta_d\approx 0.2\text{--}0.4\ \text{Gy}$ . Thus, whereas in the absence of the tethered state data, it may have been plausible to postulate  $\alpha_{HR\gamma}/\beta_{HR}\approx \alpha_d/\beta_d$ , in its presence, such assumptions are clearly inappropriate. The significance of this is that assuming  $\alpha_{HR\gamma}/\beta_{HR}\approx \alpha_d/\beta_d$  would have led to substantially lower low-dose PTC risk estimates than  $\alpha_{HR\gamma}/\beta_{HR}\approx 7\ \text{Gy}$ .

Using LSS data and the *H4-to-RET* distance data, we predict that the number of PTC target cells is of the order of  $\sim 10^6$  to  $\sim 10^7$  cells (Table 1). Compared to estimates of the total number of thyroid follicular cells,  $\sim 5\times 10^9$  cells in adults, estimated as the average number of thyroid follicular cells obtained from 1 g of adult thyroid tissue multiplied by the average weight of the adult thyroid (Nikiforov et al., unpublished results), PTC target cells comprise only a fraction of all follicular cells in the thyroid gland. Based on this, it is tempting to speculate that PTC target cells might be thyroid stem cells, or, more likely, a fraction of thyroid cells with certain growth or functional characteristics. Although currently there is no convincing evidence that thyroid stem cells exist, it is well established that thyroid follicular cells are heterogeneous with respect to their functional and proliferative qualities, including thyroglobulin production, iodine transport and organification, as well as spontaneous and thyrotropin-stimulated growth [44].

For the LSS data set, excess absolute risk (EAR) estimates of 4.3, 2.7 and 0.21 per  $10^4\ \text{PY Sv}$  were previ-

ously observed for ages at exposure of <10 y, 10–20 y, and >20 y, respectively [29]. In our model,  $\lambda_1$  did not differ significantly from zero ( $P>0.5$ ), and because of its magnitude,  $-0.0044 \text{ y}^{-1}$ , it contributes essentially trivially to the model fit;  $\lambda_2$  did differ significantly from ( $P<0.03$ ). This finding suggests that the age-at-exposure dependence previously observed for thyroid cancer [29] is perhaps due to an *H4-RET*-independent PTC induction pathway, i.e. a pathway corresponding to the delayed dose-response component in Eq. (6).

Epidemiological models other than Eq. (6) are also possible. For example, a two-stage clonal expansion model was recently fitted to thyroid cancer incidence following the Chernobyl accident [45]. Fitting the LSS incidence data to two- and three-stage clonal expansion models [46], we found target cell number estimates to be unrealistic in childhood years ( $\sim 10^{15}$  cells for males and females for the two-mutation model,  $\sim 10^{24}$  cells for males and females for the three-mutation model) but perhaps plausible for adulthood ( $\sim 10^4$  cells).

High-dose RT-PCR data [47, 48, 49, 50] suggest that radiation induction of *BCR-ABL* is about as frequent per cell as induction of *H4-RET*. Assuming a marrow dose to A-bomb survivors that is about 75% the thyroid dose, one can approximately predict the number of PTC target cells as being equal to the number of radiation-induced PTCs divided by the number of radiation-induced chronic myeloid leukemias (CML), multiplied by 0.75, multiplied by the number of CML target cells, which we assume to be  $10^7$  [3]. Focusing just on Hiroshima males, for reasons described elsewhere [51], and focusing further on individuals exposed before the age of 20, we find 4 cases of CML that are likely to be radiation-induced since their times since exposure are less than 15 years, and we find 4 thyroid cancers (assumed to be PTCs), at least 3 of which are likely to be radiation-induced since, based on person-years, only 0.7 are expected. The number of PTC target cells in Hiroshima male children can therefore be predicted to be approximately  $(3/4)(0.75)(1 \times 10^7) = 0.5 \times 10^7$  cells, completely consistent with the results in Table 1. In this calculation, we note that follow-up of CML began 5.1 years after the exposure, whereas follow-up of thyroid cancer began only after 12.4 years. Although only the ratio of radiation-induced cases matters here (and thus differences in endpoint time scales might provide some fortuitous compensation for the differential delay in follow-up), the delay could still adversely affect this calculation – experience from Chernobyl-exposed groups [52, 53, 54] indicates that substantial numbers of radiation-induced thyroid cancers would be expected in the period between 5.1 and 12.4 years after exposure.

In the limit of low-doses of  $\gamma$ -rays, and in the absence of competing risks, the lifetime excess absolute risk of *H4-RET* mediated PTC is  $R_\gamma = \alpha_{hr\gamma} N$ . Thus, each estimate of  $N$  in Table 1 can be assigned an associated estimate of  $R_\gamma$  (not shown): the first two rows (RBE=20) have the same  $R_\gamma$  (changes in  $\alpha_{hr\gamma}$  are offset by changes in  $N$ ), the third row (RBE=5) has a slightly higher  $R_\gamma$  and the

fourth row (RBE=80) has an  $R_\gamma$  that is about 50% that of the other rows (at this RBE neutrons account for a sizable fraction of the PTC risk). In a previous paper [3], knowing the order of magnitude of  $N$  for CML ( $\sim 10^7$  based on hematological considerations) was enough to favor some of the  $R_\gamma$  estimates more so than others. Here, since we have no biological estimates of  $N$  for PTC, we have no external basis for judging our results (save the “parallelogram” approach of the previous paragraph).

It is anticipated that further follow-up of the Japanese atomic bomb survivors from 1987 onwards will help to clarify whether or not the increase in EAR seen after 35 years of exposure (Fig. 2) is indeed real. If it is real, and if the *H4-RET* (*RET/PTC1*) prevalence is excessive in newly arriving PTC cases, then our modeling assumptions are incorrect and our predictions thus nullified. On the other hand, if the EAR increase does not continue, or if it does but the *H4-RET* (*RET/PTC1*) prevalence in newly arriving PTC cases is no different from the background prevalence, then perhaps Eq. (6) is reasonable.

Target cells are defined here as follicular thyroid cells that have the potential of forming *H4-RET* mediated radiation-induced PTC. One can hypothesize, however, that if the key feature of target cells is their potential to proliferate, common target cells may exist for all pathways to PTC. To test this one could: (a) measure *ELE1-RET* distances in thyroid cells to predict  $\alpha_{er}$ , (b) using data that includes immediate follow up (i.e. data described in [1] or the Chernobyl data), resolve radiation-induced thyroid cancers into a rapid component for *ELE1-RET* (*RET/PTC3*)-mediated cases and a slower component for *H4-RET* (*RET/PTC1*)-mediated cases, and (c) check to see if the resulting estimates of  $N$  and  $\lambda$  are approximately the same for both pathways.

**Acknowledgments** We thank the reviewers for suggestions and Dr. J. Chen for sharing her results on  $t(r)$ . This publication was supported in part by funds from NIH GMS 57245-03 (TR), NIH CA86823 (RKS), DE-FG03-00ER62909 from the U.S. Department of Energy (RKS), the University of Cincinnati Center for Environmental Genetics Pilot Project Grant and American Cancer Society Institutional Research Grant (YEN), and European Commission contract FIGD-CT-2000-0079 (MPL). This report makes use of data obtained from the Radiation Effects Research Foundation (RERF) in Hiroshima, Japan. RERF is a private foundation funded equally by the Japanese Ministry of Health and Welfare and the U.S. Department of Energy through the U.S. National Academy of Sciences. The conclusions in this report are those of the authors and do not necessarily reflect the scientific judgment of RERF or its funding agencies.

## References

1. Nikiforova MN, Stringer JR, Blough R, Medvedovic M, Fagin JA, Nikiforov YE (2000) Proximity of chromosomal loci that participate in radiation-induced rearrangements in human cells. *Science* 290:138–141
2. Kozubek S, Lukasova E, Mareckova A, Skalnikova M, Kozubek M, Bartova E, Kroha V, Krahulcova E, Slotova J (1999) The topological organization of chromosomes 9 and 22 in cell nuclei has a determinative role in the induction of t(9, 22) translocations and in the pathogenesis of t(9, 22) leukemias. *Chromosoma* 108:426–435

3. Radivoyevitch T, Kozubek S, Sachs RK (2001) Biologically-based risk estimation for radiation-induced CML: inferences from *BCR* and *ABL* geometric distributions. *Radiat Environ Biophys* 40:1–9
4. Ron E, Lubin JH, Shore RE, Mabuchi K, Modan B, Pottern LM, Schneider AB, Tucker MA, Boice JD Jr (1995) Thyroid cancer after exposure to external radiation: a pooled analysis of seven studies. *Radiat Res* 141:259–277
5. Kazakov VS, Demidchik EP, Astakhova LN (1992) Thyroid cancer after Chernobyl. *Nature* 359:21
6. Likhtarev IA, Sobolev BG, Kairo IA, Tronko ND, Bogdanova TI, Oleinic VA, Epshtein EV, Beral V (1995) Thyroid cancer in the Ukraine. *Nature* 375:365
7. Cotran RS, Kumar V, Robbins SL (1994) Pathological basis of disease. WB Saunders, Philadelphia
8. Negri E, Ron E, Franceschi S, Dal Maso L, Mark SD, Preston-Martin S, McTiernan A, Kolonel L, Kleinerman R, Land C, Jin F, Wingren G, Galanti MR, Hallquist A, Glattre E, Lund E, Levi F, Linos D, Braga C, La Vecchia C (1999) A pooled analysis of case-control studies of thyroid cancer. I. Methods. *Cancer Causes Control* 10:131–142
9. Shore RE (1992) Issues and epidemiological evidence regarding radiation-induced thyroid cancer. *Radiat Res* 131:98–111
10. Grieco M, Santoro M, Berlingieri MT, Melillo RM, Donghi R, Bongarzone I, Pierotti MA, Della PG, Fusco A, Vecchio G (1990) PTC is a novel rearranged form of the ret proto-oncogene and is frequently detected in vivo in human thyroid papillary carcinomas. *Cell* 60:557–563
11. Bongarzone I, Butti MG, Coronelli S, Borrello MG, Santoro M, Mondellini P, Pilotti S, Fusco A, Della PG, Pierotti MA (1994) Frequent activation of ret protooncogene by fusion with a new activating gene in papillary thyroid carcinomas. *Cancer Res* 54:2979–2985
12. Santoro M, Dathan NA, Berlingieri MT, Bongarzone I, Paulin C, Grieco M, Pierotti MA, Vecchio G, Fusco A (1994) Molecular characterization of RET/PTC3; a novel rearranged version of the RET proto-oncogene in a human thyroid papillary carcinoma. *Oncogene* 9:509–516
13. Zou M, Shi Y, Farid NR (1994) Low rate of ret proto-oncogene activation (PTC/retPTC) in papillary thyroid carcinomas from Saudi Arabia. *Cancer* 73:176–180
14. Mayr B, Potter E, Goretzki P, Ruschoff J, Dietmaier W, Hoang-Vu C, Dralle H, Brabant G (1998) Expression of Ret/PTC1, -2, -3, -delta3 and -4 in German papillary thyroid carcinoma. *Br J Cancer* 77:903–906
15. Motomura T, Nikiforov YE, Namba H, Ashizawa K, Nagataki S, Yamashita S, Fagin JA (1998) Ret rearrangements in Japanese pediatric and adult papillary thyroid cancers. *Thyroid* 8:485–489
16. Tallini G, Ghossein RA, Emanuel J, Gill J, Kinder B, Dimich AB, Costa J, Robbins R, Burrow GN, Rosai J (1998) Detection of thyroglobulin, thyroid peroxidase, and RET/PTC1 mRNA transcripts in the peripheral blood of patients with thyroid disease. *J Clin Oncol* 16:1158–1166
17. Fugazzola L, Pilotti S, Pinchera A, Vorontsova TV, Mondellini P, Bongarzone I, Greco A, Astakhova L, Butti MG, Demidchik EP (1995) Oncogenic rearrangements of the RET proto-oncogene in papillary thyroid carcinomas from children exposed to the Chernobyl nuclear accident. *Cancer Res* 55:5617–5620
18. Klugbauer S, Lengfelder E, Demidchik EP, Rabes HM (1995) High prevalence of RET rearrangement in thyroid tumors of children from Belarus after the Chernobyl reactor accident. *Oncogene* 11:2459–2467
19. Bounacer A, Wicker R, Schlumberger M, Sarasin A, Suarez HG (1997) Oncogenic rearrangements of the ret proto-oncogene in thyroid tumors induced after exposure to ionizing radiation. *Biochimie* 79:619–623
20. Bounacer A, Wicker R, Caillou B, Cailleux AF, Sarasin A, Schlumberger M, Suarez HG (1997) High prevalence of activating ret proto-oncogene rearrangements, in thyroid tumors from patients who had received external radiation. *Oncogene* 15:1263–1273
21. Powell DJ Jr, Russell J, Nibu K, Li G, Rhee E, Liao M, Goldstein M, Keane WM, Santoro M, Fusco A, Rothstein JL (1998) The RET/PTC3 oncogene: metastatic solid-type papillary carcinomas in murine thyroids. *Cancer Res* 58:5523–5528
22. Nikiforov YE, Rowland JM, Bove KE, Monforte-Munoz H, Fagin JA (1997) Distinct pattern of ret oncogene rearrangements in morphological variants of radiation-induced and sporadic thyroid papillary carcinomas in children. *Cancer Res* 57:1690–1694
23. Thomas GA, Bunnell H, Cook HA, Williams ED, Nerovnya A, Cherstvoy ED, Tronko ND, Bogdanova TI, Chiappetta G, Viglietto G, Pentimalli F, Salvatore G, Fusco A, Santoro M, Vecchio G (1999) High prevalence of RET/PTC rearrangements in Ukrainian and Belarussian post-Chernobyl thyroid papillary carcinomas: a strong correlation between RET/PTC3 and the solid-follicular variant. *J Clin Endocrinol Metab* 84:4232–4238
24. Smida J, Salassidis K, Hieber L, Zitzelsberger H, Kellerer AM, Demidchik EP, Negele T, Spelsberg F, Lengfelder E, Werner M, Bauchinger M (1999) Distinct frequency of ret rearrangements in papillary thyroid carcinomas of children and adults from Belarus. *Int J Cancer* 80:32–38
25. Rabes HM, Demidchik EP, Sidorow JD, Lengfelder E, Beimfohr C, Hoelzel D, Klugbauer S (2000) Pattern of radiation-induced RET and NTRK1 rearrangements in 191 post-Chernobyl papillary thyroid carcinomas: biological, phenotypic, and clinical implications. *Clin Cancer Res* 6:1093–1103
26. Santoro M, Chiappetta G, Cerrato A, Salvatore D, Zhang L, Manzo G, Picone A, Portella G, Santelli G, Vecchio G, Fusco A (1996) Development of thyroid papillary carcinomas secondary to tissue-specific expression of the RET/PTC1 oncogene in transgenic mice. *Oncogene* 12:1821–1826
27. Jhiang SM, Sagartz JE, Tong Q, Parker-Thornburg J, Capen CC, Cho JY, Xing S, Ledent C (1996) Targeted expression of the ret/PTC1 oncogene induces papillary thyroid carcinomas. *Endocrinology* 137:375–378
28. Viglietto G, Chiappetta G, Martinez-Tello FJ, Fukunaga FH, Tallini G, Rigopoulou D, Visconti R, Mastro A, Santoro M, Fusco A (1995) RET/PTC oncogene activation is an early event in thyroid carcinogenesis. *Oncogene* 11:1207–1210
29. Thompson DE, Mabuchi K, Ron E, Soda M, Tokunaga M, Ohikubo S, Sugimoto S, Ikeda T, Terasaki M, Izumi S, Preston DL (1994) Cancer incidence in atomic bomb survivors. Part II: Solid tumors, 1958–1987. *Radiat Res* 137:S17–S67
30. Kellerer AM, Rossi HH (1978) A generalized formulation of dual radiation action. *Radiat Res* 75:471–488
31. Grieco M, Cerrato A, Santoro M, Fusco A, Melillo RM, Vecchio G (1994) Cloning and characterization of H4 (D10S170), a gene involved in RET rearrangements in vivo. *Oncogene* 9:2531–2535
32. Morton NE (1991) Parameters of the human genome. *Proc Natl Acad Sci USA* 88:7474–7476
33. Löbrich M, Ikpeme S, Kiefer J (1994) Measurement of DNA double-strand breaks in mammalian cells by pulsed-field gel electrophoresis: a new approach using rarely cutting restriction enzymes. *Radiat Res* 138:186–192
34. Cedervall B, Wong R, Albright N, Dynlacht J, Lambin P, Dewey WC (1995) Methods for the quantification of DNA double-strand breaks determined from the distribution of DNA fragment sizes measured by pulsed-field gel electrophoresis. *Radiat Res* 143:8–16
35. Sachs RK, van den Engh G, Trask B, Yokota H, Hearst JE (1995) A random-walk/giant-loop model for interphase chromosomes. *Proc Natl Acad Sci USA* 92: 2710–2714
36. ICRP (1991) 1990 Recommendations of the International Commission on Radiological Protection. *Annals of the ICRP* 21:1–3
37. McCullagh P, Nelder JA (1989) Generalized linear models. Chapman and Hall/CRC, Boca Raton

38. MATLAB version 6 (2000) Mathworks Inc., Natick, MA
39. Preston DL, Lubin JH, Pierce DA, McConney ME (1998) *Epicure Release 2.10*. HiroSoft International, Seattle
40. Chen J, Nekolla E, Kellerer AM (1996) A comparative study of microdosimetric properties of x-rays, gamma-rays, and beta-rays. *Radiat Environ Biophys* 35:263–266
41. Lloyd DC, Edwards AA (1983) Chromosome aberrations in human lymphocytes: effect of radiation quality, dose, and dose rate. In: Ishihara T, Sasaki M (eds) *Radiation-induced chromosome damage in man*. Liss, New York, pp 23–49
42. Preston DL, Kusumi S, Tomonaga M, Izumi S, Ron E, Kuramoto A, Kamada N, Dohy H, Matsuo T, Nonaka H, Thompson DE, Soda M, Mabuchi K (1994) Cancer incidence in atomic bomb survivors. Part III. Leukemia, lymphoma and multiple myeloma, 1950–1987. *Radiat Res* 137:S68–S97
43. Bauchinger M, Schmid E, Streng S, Dresch J (1983) Quantitative analysis of the chromosome damage at first division of human lymphocytes after <sup>60</sup>CO gamma-irradiation. *Radiat Environ Biophys* 22:225–229
44. Studer H, Peter HJ, Gerber H (1989) Natural heterogeneity of thyroid cells: the basis for understanding thyroid function and nodular goiter growth. *Endocr Rev* 10:125–135
45. Leenhouts HP, Brugmans MJ, Chadwick KH (2000) Analysis of thyroid cancer data from the Ukraine after 'Chernobyl' using a two-mutation carcinogenesis model. *Radiat Environ Biophys* 39:89–98
46. Little MP (1995) Are two mutations sufficient to cause cancer? Some generalizations of the two-mutation model of carcinogenesis of Moolgavkar, Venzon, and Knudson, and of the multistage model of Armitage and Doll. *Biometrics* 51:1278–1291
47. Ito T, Seyama T, Iwamoto KS, Hayashi T, Mizuno T, Tsuyama N, Dohi K, Nakamura N, Akiyama M (1993) In vitro irradiation is able to cause RET oncogene rearrangement. *Cancer Res* 53:2940–2943
48. Ito T, Seyama T, Mizuno T, Hayashi T, Iwamoto KS, Dohi K, Nakamura N, Akiyama M (1993) Induction of BCR-ABL fusion genes by in vitro X-irradiation. *Jpn J Cancer Res* 84:105–109
49. Mizuno T, Kyoizumi S, Suzuki T, Iwamoto KS, Seyama T (1997) Continued expression of a tissue specific activated oncogene in the early steps of radiation-induced human thyroid carcinogenesis. *Oncogene* 15:1455–1460
50. Mizuno T, Iwamoto KS, Kyoizumi S, Nagamura H, Shinohara T, Koyama K, Seyama T, Hamatani K (2000) Preferential induction of RET/PTC1 rearrangement by X-ray irradiation. *Oncogene* 19:438–443
51. Radivoyevitch T, Hoel DG (2000) Biologically-based risk estimation for radiation-induced chronic myeloid leukemia. *Radiat Environ Biophys* 39:153–159
52. Williams D, Pinchera A, Karaoglou A, Chadwick KH (1993) Thyroid cancer in children living near Chernobyl. Expert panel report on the consequences of the Chernobyl accident. EUR 15248 EN
53. Williams ED, Becker D, Dimichik EP, Nagataki S, Pinchera A, Tronko ND (1996) Effects on the thyroid in populations exposed to radiation as a result of the Chernobyl accident. In: *One decade after Chernobyl. Summing up the consequences of the accident. Proceedings of an international conference on One decade after Chernobyl. Summing up the consequences of the accident*. IAEA, Vienna, pp 207–238
54. Sobolev B, Heidenreich WF, Kairo I, Jacob P, Goulko G, Likhtarev I (1997) Thyroid cancer incidence in the Ukraine after the Chernobyl accident: comparison with spontaneous incidences. *Radiat Environ Biophys* 36:195–199